

# Investigating the relationship between local climate zone and land surface temperature

- A case study in Shanghai

Meng CAI, Chao REN, Yong XU  
Institute of Future Cities (IOFC),  
The Chinese University of Hong Kong,  
Hong Kong, China  
caimeng@cuhk.edu.hk

**Abstract**—The concept of Local Climate Zone (LCZ) has been developed to quantify the correlation between urban morphology and urban heat island (UHI). Each LCZ is supposed to have homogenous air temperature. However, traditional air temperature observation methods have limited spatial coverage and poor spatial resolution. Land surface temperature (LST) acquired from satellite images can be used to study the temperature characteristics of LCZ classes by providing continuous data on surface temperature. This study aims to study the relationship between LST and LCZ classes with Shanghai selected as a case study because of its high urbanization rate and serious UHI effect. This study has three major steps: Firstly, Shanghai local climate zone map was generated using the World Urban Database and Portal Tool (WUDAPT) method. Secondly, a remote sensing approach was taken to acquire Shanghai's LST from night-time Aster thermal data in different seasons. Thirdly, the LST was associated with the Shanghai LCZ map and the correlation between LCZ and LST in Shanghai was discussed.

The results show that there are large variations in LST across LCZ classes in different months in Shanghai. These results will be able to offer integrated information under urban climate principles for urban planners and urban climate researchers.

**Keywords**—local climate zone; land surface temperature; WUDAPT; Aster.

## I. INTRODUCTION

Rapid urban developments in China have not only changed natural landscapes into artificial constructions and pavements, but also brought along many environmental problems, such as the urban heat island (UHI) effect. Therefore, the study of UHI and its pattern has been a continuous pursuit for climatologists and urban planners. For this purpose, the concept of Local Climate Zone (LCZ) has been developed to quantify the correlation between urban morphology and UHI [1]. The World Urban Database and Portal Tool (WUDAPT) is a newly developed approach to realize the LCZ classification using freely available data and software[2].

Each LCZ is supposed to represent homogenous air temperature. However, traditional air temperature observation methods have limited spatial coverage and poor spatial resolution. Therefore, alternative temperature data is necessary for more comprehensive assessment of the effect of urban morphology on local climatic conditions. Satellite image can

reveal the urban thermal environment by providing continuous coverage, high integrity and real-time data acquisition over large areas[3]. In addition, satellite imagery obtained during night time would result in a stronger relationship between the surface and the adjacent air[4, 5]. Thus, night-time satellite imagery may provide a representation of air temperatures accurate enough for UHI studies at city scale[6].

This study aims to determine the relationship between LST and LCZ. The WUDAPT method was applied to create LCZ maps of Shanghai. LST of Shanghai was acquired using nighttime Aster images in different seasons. LST in each LCZ can therefore be characterized to provide urban climate researchers and urban planners information about the influence of LCZ on local climate, leading to more sustainable urban planning in Chinese cities.

## II. REVIEW

### A. Local Climate Zone (LCZ)

Steward and Oke developed the Local Climate Zones to characterize cities in a comprehensive and standardized way[1]. Each LCZ aims to have homogenous air temperature and is defined by both qualitative and quantitative properties. One of the major advantages of LCZ is the new perspective to evaluate urban heat island, looking into the temperature differences among LCZ classes rather than the traditional “urban” and “rural” classes. It emphasized the importance of intra-urban temperature comparison among different urban classes, to analyze the influence of heterogeneous urban morphology on local climate formation. The LCZ classification has 17 standard types (Table 1).

TABLE I. NAMES AND DESIGNATION OF THE LCZ TYPES [1]

Built types	Land cover types
LCZ1: Compact high-rise	LCZ A: Dense trees
LCZ2: Compact mid-rise	LCZ B: Scattered trees
LCZ3: Compact low-rise	LCZ C: Bush, scrub
LCZ4: Open high-rise	LCZ D: Low plants
LCZ5: Open mid-rise	LCZ E: Bare rock or paved
LCZ6: Open low-rise	LCZ F: Bare soil or sand
LCZ7: Lightweight low-rise	LCZ G: Water
LCZ8: Large low-rise	
LCZ9: Sparse low-rise	
LCZ10: Heavy industry	

### B. World Urban Database and Portal Tool (WUDAPT)

WUDAPT targets to be part of a global protocol to derive information about form and function of cities. It is designed according to the requirements of universality, free availability of data and software, objectivity, computational costs, and straightforward to apply[2]. Based on these requirements, a standard workflow has been developed, which makes use of free Landsat 8 images, free software: SAGA GIS and Google Earth (GE) and Random Forest classifier.

## III. METHODOLOGY

### A. Study Area

Shanghai (30°40'N~31°53'N, 120°51'E~122°12'E) is located on the alluvial terrace of the Yangtze River delta.

TABLE II. THE CLIMATE CHARACTER OF SHANGHAI

Area	Climatic Region	Terrain	Ave. temp	Annual rainfall	Extreme high temp	Ave. high temp
6340.5 km <sup>2</sup>	Humid subtropical climate	plain with a few hilly area	17.1°C	1166.1 mm	39.9°C	20.6 °C

Shanghai has the highest population density in China and is one of the most vigorous economic zones in the world, with 1717 billion Chinese Yuan of gross domestic product (GDP) in 2010 [7], accounting for 4.3% of China's total amount. It is divided into 18 county-level divisions: 17 districts and one county (Fig. 1), of which 9 districts in the core of city are collectively referred to as urban areas. The downtown area is located in the middle and south of the city.

Shanghai has experienced drastic urban development since China's economic reform in the early 1980s. The fast urban development of Shanghai has led to an intensified urban heat island effect. Previous climate studies in Shanghai show that urban areas have higher air temperature, more hot days, lower relative humidity and lower wind speed than rural areas. [8, 9].

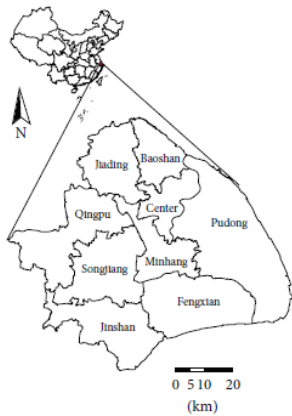


Fig. 1. location of the study area[9]

### B. Data

Landsat 8 level 1 image (4-Nov-14) of Shanghai with resolution of 30m was downloaded from the USGS (U.S. Geological Survey) due to the little cloud coverage. The original band of the Landsat data were used in the classification process.

Night-time Aster thermal data at different time (17-Jan-14, 23-Oct-14, 01-Sep-15) were downloaded from NASA to acquire LST. The three dates are winter, fall and summer in Shanghai respectively and are selected to represent the seasonality variation of LST.

### C. Research Steps

Firstly, the WUDAPT method is applied to generate LCZ maps.

There are main four steps in this study following the WUDAPT method [2, 10]:

(a) Pre-processing of Landsat data: the selected Landsat image was clipped by the city's boundary in order to decrease the computation time. This pre-processed image was resampled into 100 meters to get a representation of the spectral signal of local-scale urban structures rather than smaller objects.

(b) Digitization of training areas in GE according to the LCZ scheme: the representative areas of each LCZ class area were selected by polygons as training samples and saved in a kml format. Each LCZ contains about 20 training samples.

(c) Classification in SAGA-GIS: the pre-processed Landsat images and the selected training areas were input into SAGA-GIS. The LCZ classification of study areas was calculated and conducted by the random forest classifier based on similarities between the training samples and the rest of study areas.

(d) Accuracy assessment: The GE image was regarded as the reference data, which is believed to be accurate enough to reflect the true land-cover to validate the classification result. Validation samples extracted from the GE image were used to validate the LCZ map and each LCZ contained about 5 samples. The results of an accuracy assessment were summarized in a confusion matrix. The degree of confusion between the classification result and the ground truth can be calculated in the matrix.

Secondly, the night-time Aster thermal images were converted into LST using the single channel algorithm. The band 13 of the Aster image was selected for calculation.

- the digital number (DN) values of the Aster image band 13 were converted to radiance ( $L_{sen}$ ) using the unit conversion coefficient of  $5.69 \times 10^{-3}$  [11].
- black body temperature was computed using equation (1) derived from the inversion of Plank's function[12]:

$$T_{sen} = \frac{K_2}{\ln\left(\frac{K_1}{L_{sen}} + 1\right)} \quad (1)$$

$$\gamma \approx \frac{T_{sen}^2}{K_2 L_{sen}} \quad (2)$$

$$\delta \approx T_{sen} - \frac{T_{sen}^2}{K_2} \quad (3)$$

where  $K_1$  and  $K_2$  are radiation constants. For band 13,  $K_1=865.25W \cdot m^{-2} \cdot sr^{-1} \cdot \mu m^{-1}$ ,  $K_2=1349.82K$ .  $\gamma$  and  $\delta$  are two parameters dependent on the Planck's function.

- (c) Surface emissivity ( $\epsilon$ ) was retrieved using the NDVI[13]. The surface emissivity for band 13 was calculated using (5):

$$P_V = \left( \frac{NDVI - NDVI_S}{NDVI_V - NDVI_S} \right)^2 \quad (4)$$

$$\epsilon = 0.986 + 0.022P_V \quad (5)$$

where  $NDVI_V$  and  $NDVI_S$  are the NDVI values of full vegetation cover ( $P_V = 1$ ) and bare soil ( $P_V = 0$ ), respectively.

- (d) The single channel algorithm retrieved LST using the following general equation[14]:

$$T_s = \gamma \left[ \frac{1}{\epsilon} (\psi_1 L_{sen} + \psi_2) + \psi_3 \right] + \delta \quad (6)$$

where  $T_s$  is the LST,  $\epsilon$  is the surface emissivity, and  $\psi_1$ ,  $\psi_2$ , and  $\psi_3$  are referred to as atmospheric functions.

Finally, the mean LST in each LCZ was calculated by zonal statistic on the platform of ArcGIS in order to obtain quantified comparison between LST and LCZ.

#### IV. RESULTS AND ANALYSIS

##### A. Results

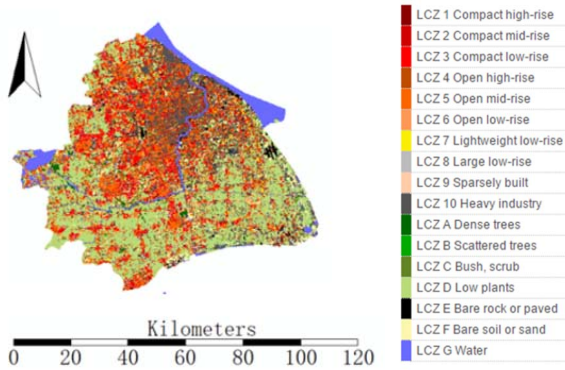


Fig. 2. Shanghai LCZ map

TABLE III. CONFUSION MATRIX OF SHANGHAI LCZ MAP

LCZ	1	2	3	4	5	6	7	8	9	10	A	B	C	D	E	F	G	$\Sigma$	UA
1	1	0	0	5	1	0	1	1	0	0	0	0	0	0	0	0	0	9	11%
2	1	4	5	4	1	0	3	0	0	0	0	0	0	0	0	0	0	18	22%
3	0	5	42	5	0	2	2	5	0	2	0	0	0	1	6	0	0	70	60%
4	1	1	0	30	8	7	0	0	0	0	2	0	0	16	0	0	0	65	46%
5	0	4	2	4	4	3	2	1	0	0	0	0	0	5	1	0	0	26	15%
6	0	1	0	4	6	35	1	0	0	0	2	0	0	21	0	2	0	72	49%
7	1	3	6	0	0	2	8	0	0	0	0	0	0	4	0	0	0	24	33%
8	0	0	5	1	0	1	0	24	0	1	0	0	0	0	2	1	0	35	69%
9	0	0	0	0	0	0	0	0	2	0	0	0	0	0	0	0	0	2	100%
10	4	4	7	24	3	4	2	3	0	2	0	1	0	66	1	5	2	128	2%
A	0	0	0	2	0	0	1	0	0	0	14	1	0	0	0	0	0	18	78%
B	0	0	0	0	0	3	0	0	0	0	0	1	0	7	0	1	0	12	8%
C	0	0	0	0	0	1	0	0	0	0	0	2	3	11	0	2	0	19	16%
D	0	0	0	2	0	1	1	0	2	1	0	0	2	295	1	0	0	305	97%
E	0	0	7	1	0	0	0	12	0	0	0	0	0	3	32	2	0	57	56%
F	0	0	0	0	0	0	0	0	1	0	1	0	0	77	0	4	0	83	5%
G	0	0	0	0	1	0	0	0	0	0	0	0	0	4	0	0	939	944	99%
$\Sigma$	8	22	74	82	24	59	21	46	5	6	19	5	5	510	43	17	941	OA:76%	
PA	12%	18%	57%	37%	17%	59%	38%	52%	40%	33%	74%	20%	60%	58%	74%	24%	100%	Kappa:0.66	

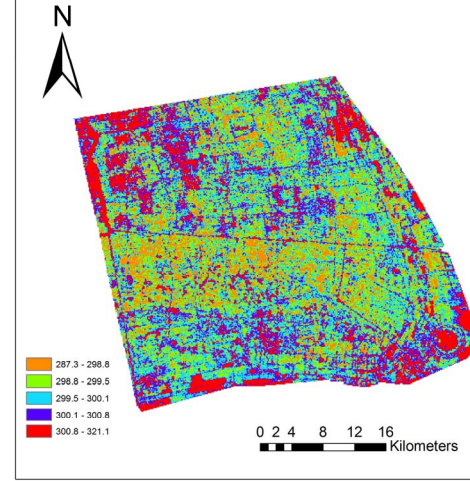


Fig. 3. Shanghai LST in summer

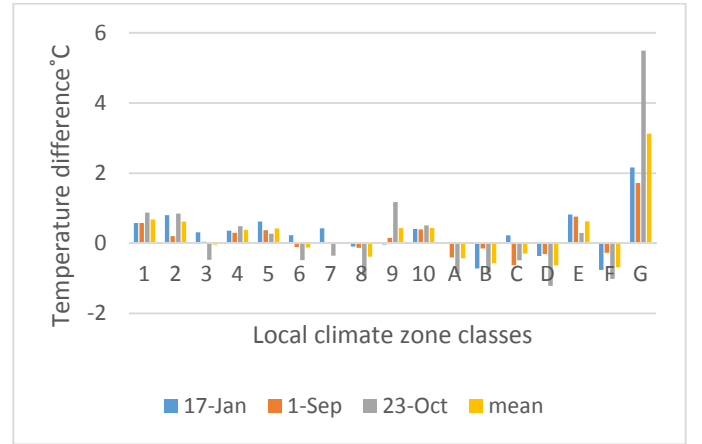


Fig. 4. Thermal differentiation of local climate zones (°C)

##### B. Analysis

Fig. 2 is the LCZ map of Shanghai Municipality area. It can capture the morphological characteristics of rural and urban areas and detect the potential UHI distribution pattern of Shanghai. Shanghai is highly urbanized with large areas classified as built-up LCZs according to the LCZ maps. Downtown areas of Shanghai Municipality, especially Center

district, are extremely dense and compact and are mainly classified into LCZs 1-4, which show the potential high UHI intensity. There is no obvious gap between the downtown area and the suburbs, representing the highly urbanization and a large area of potential UHI distribution in Shanghai.

Based on accuracy assessment steps, the confusion matrix of Shanghai LCZ map is created (Table 3). The overall accuracy of the LCZ map is 76% and the Kappa coefficient is 0.66. The accuracy assessment demonstrates a satisfying result for the large-scale classification. However, the samples in some classes such as LCZ 1, LCZ 9 and LCZ 10 only has a few pixels thus quality rates may not be very significant for these classes.

Fig. 3 is the LST map generated from night-time Aster thermal image on 01-Sep. 2015. The LST map identifies hot areas in the downtown areas in the middle and north of Shanghai. It is also noted that large areas of high temperature occurred in the suburbs to the south.

From Fig. 4, it can be observed that there is large LST variation across LCZ classes. LSTs in different time have a consistent variation of each LCZ. The built-up LCZs (1-10) are generally above the average LST while the land coverings LCZs (A-F) are below the average. Urban areas are generally hotter than rural areas, and may be an indication of the UHI effect in Shanghai. In particular, LCZ 1 (compact high-rise) has the highest LST among the built-up LCZs. There is a declining trend of LST from LCZ 1 to LCZ 6. The LCZs 7-9 have much variations in the three seasons. This may be due to the complex and diverse urban morphology of these LCZs in Shanghai, resulting in great temperature differences within the LCZ classes. LCZ E (Bare rock/paved) is a land covering LCZ above the average LST. Some of the LCZ E in Shanghai represent the airport and areas built up with concrete and steel, so they may have similar thermal characteristics with the built-up LCZs. LCZ D has the lowest LST among all the LCZs. LCZ G (water) in Shanghai has the highest LST due to its highest heat capacity. It cools off slower than other land types at night.

## V. CONCLUSION

The Shanghai LCZ maps generated by the WUDAPT method can effectively capture the city's urban morphology and potentially reveal the UHI situation. Although the concept of LCZ classification scheme is based on measurements of air temperature, LST was found to be associated with LCZ classes by comparing the LST and LCZ in Shanghai. The built-up LCZs have higher LST than land covering LCZs in general. Also, LST declines from LCZ 1 to LCZ 6 and LCZ D has the lowest LST. The complex urban morphology in Shanghai leads to some inconsistency of LSTs in LCZs 7-9.

The findings of this study can help urban planners and urban climate researchers better understand the influence of urban morphology on local climatic conditions. Results can also be used as a reference to assist climate-sensitive urban planning, eco-city evaluation and heat wave studies. Further study is needed to focus on other cities to have a more comprehensive understanding on the correlation between LST and LCZ.

## References

- [1] I. D. Stewart and T. R. Oke, "Local Climate Zones for Urban Temperature Studies," *Bulletin of the American Meteorological Society*, vol. 93, pp. 1879-1900, 2012.
- [2] B. Bechtel, P. Alexander, J. Böhner, J. Ching, O. Conrad, J. Feddema, G. Mills, L. See, and I. Stewart, "Mapping Local Climate Zones for a Worldwide Database of the Form and Function of Cities," *ISPRS International Journal of Geo-Information*, vol. 4, pp. 199-219, 2015.
- [3] D. Streutker, "Satellite-measured growth of the urban heat island of Houston, Texas," *Remote Sensing of Environment*, vol. 85, pp. 282-289, 2003.
- [4] J. A. Voogt and T. R. Oke, "Thermal remote sensing of urban climates," *Remote Sensing of Environment*, vol. 86, pp. 370-384, 2003.
- [5] M. J. Stoll, & Brazel, A. J., "Surface-air temperature relationships in the urban environment of Phoenix, Arizona," *Physical Geography*, vol. 13(2), pp. 160-179, 1992.
- [6] J. E. Nichol and P. H. To, "Temporal characteristics of thermal satellite images for urban heat stress and heat island mapping," *ISPRS Journal of Photogrammetry and Remote Sensing*, vol. 74, pp. 153-162, 2012.
- [7] S. M. S. Bureau, *Shanghai Statistical Yearbook 2000-2011*. Beijing: China Statistics Press, 2011.
- [8] L. Cui and J. Shi, "Urbanization and its environmental effects in Shanghai, China," *Urban Climate*, vol. 2, pp. 1-15, 2012.
- [9] L. Chen, R. Jiang, and W.-N. Xiang, "Surface Heat Island in Shanghai and Its Relationship with Urban Development from 1989 to 2013," *Advances in Meteorology*, vol. 2016, pp. 1-15, 2016.
- [10] C. Ren, M. Cai, R. Wang, Y. Xu, and E. Ng, "Local Climate Zone (LCZ) Classification by using the method of World Urban World Urban Database and Access Portal Tools (WUDAPT): A Case Study in Wuhan and Hangzhou," presented at the The Fourth International Conference on Countermeasure to Urban Heat Islands (4th IC2UHI), Singapore, 2016.
- [11] ERSDAC. (2010). ASTER GDS. Available: [http://www.gds.aster.ersdac.or.jp/gds\\_www2002/exhibition\\_e/a\\_sensor\\_e/set\\_a\\_sensor\\_e.html](http://www.gds.aster.ersdac.or.jp/gds_www2002/exhibition_e/a_sensor_e/set_a_sensor_e.html)
- [12] J. C. J.-M. a. J. A. Sobrino, "A Single-Channel Algorithm for Land-Surface Temperature Retrieval From ASTER Data," *IEEE Geoscience and Remote Sensing Letters*, vol. 7(1), pp. 176-179, 2010.
- [13] J. C. Jiménez-Muñoz, J. A. Sobrino, A. Gillespie, D. Sabol, and W. T. Gustafson, "Improved land surface emissivities over agricultural areas using ASTER NDVI," *Remote Sensing of Environment*, vol. 103, pp. 474-487, 2006.
- [14] J. C. Jiménez-Muñoz, "A generalized single-channel method for retrieving land surface temperature from remote sensing data," *Journal of Geophysical Research*, vol. 108, 2003.